

# Columnar and Laminar Segregation of Retinal Input to the Primate Superior Colliculus Revealed by Anterograde Tracer Injection Into Each Eye

Mikayla D. Dilbeck, Zachary R. Spahr, Rakesh Nanjappa, John R. Economides, and Jonathan C. Horton

Program in Neuroscience, Department of Ophthalmology, University of California, San Francisco, San Francisco, California, United States

Correspondence: Jonathan C. Horton, University of California, San Francisco, 10 Koret Way, San Francisco, CA 94143-0730, USA; [jonathan.horton@ucsf.edu](mailto:jonathan.horton@ucsf.edu).

**Received:** September 10, 2021

**Accepted:** December 11, 2021

**Published:** January 7, 2022

Citation: Dilbeck MD, Spahr ZR, Nanjappa R, Economides JR, Horton JC. Columnar and laminar segregation of retinal input to the primate superior colliculus revealed by anterograde tracer injection into each eye. *Invest Ophthalmol Vis Sci.* 2022;63(1):9. <https://doi.org/10.1167/iovs.63.1.9>

**PURPOSE.** After the lateral geniculate nucleus, the superior colliculus is the richest target of retinal projections in primates. Hubel et al. used tritium autoradiography to show that axon terminals emanating from one eye form irregular columns in the stratum griseum superficiale. Unlabeled gaps were thought to be filled by the other eye, but this assumption was never tested directly.

**METHODS.** Experiments were performed in two normal macaques. In monkey 1, [<sup>3</sup>H]proline was injected into the left eye and the pattern of radiolabeling was examined in serial cross-sections through the entire superior colliculus. In monkey 2, cholera toxin subunit B conjugated to Alexa 488 was injected into the right eye and cholera toxin subunit B - Alexa 594 was injected into the left eye. The two fluorescent labels were compared in a reconstruction of the superior colliculus prepared from serial sections.

**RESULTS.** In monkey 1, irregular columns of axon terminals were present in the superficial grey. The projection from the peripheral retina was stronger than the projection from the macula. In monkey 2, the two fluorescent Alexa tracers mainly interdigitated: a conspicuous gap in one label was usually filled by a clump of the other label. There was also partial laminar segregation of ocular inputs. In the far peripheral field representation, the contralateral eye's input generally terminated closer to the tectal surface. In the midperiphery the eyes switched, bringing the ipsilateral input nearer the surface.

**CONCLUSIONS.** Direct retinal input to the macaque superior colliculus is segregated into alternating columns and strata, despite the fact that tectal cells respond robustly to stimulation of either eye.

**Keywords:** cholera toxin subunit B, Alexa Fluor, proline autoradiography, saccade, pretectal olivary nucleus

About 10% of retinal ganglion cells project to the superior colliculus in the macaque.<sup>1</sup> Hubel et al.<sup>2</sup> labeled their axon terminals by injecting radioactive tracers into one eye. Autoradiographs showed stronger innervation of the contralateral tectum, although this bias was far less pronounced than in the cat or mouse.<sup>3,4</sup> Silver grains were concentrated in the stratum griseum superficiale, often forming clumps 100 to 500 μm wide, especially on the side ipsilateral to the injected eye. These clumps were separated by more sparsely labeled gaps approximately equal in width. It was assumed that the gaps were filled by axon terminals from the other eye, thereby forming a mosaic of alternating, mostly segregated ocular input to the superior colliculus.

This interpretation seems probable and logical, especially given the segregation of input to the other major target of the retina, the lateral geniculate nucleus. An alternative scheme, however, has never been fully ruled out: perhaps inputs from the two eyes are largely overlapping rather than interdigitated. Conceivably, the zones labeled by monocular tracer injection receive strong input from both eyes,

whereas the gaps between them receive weak input from both eyes. A single prior study attempted to resolve this issue by removing one eye and injecting a radioactive tracer into the remaining eye of the same monkey.<sup>5</sup> Degenerating axon terminals were present in the gaps between clumps of autoradiographic label, consistent with the notion that ocular inputs are dovetailed. However, degenerating terminals were also abundant in regions well-labeled via the other eye, leading the investigators to conclude that much of the superior colliculus receives coincident input from the two eyes.

To determine whether retinal input to the primate superior colliculus is mostly overlapping or interdigitated, we have taken the approach of injecting each eye with an anterogradely transported tracer: cholera toxin subunit B. In the right eye, the tracer was conjugated to Alexa Fluor 488 and in the left eye it was conjugated to Alexa Fluor 594.<sup>6,7</sup> The distribution of the two labels, identical except for their fluorophore, allowed a direct comparison of the pattern formed by each eye's projection to the superior colliculus.

## METHODS

### Animals and Experimental Procedures

Two normal male Rhesus monkeys from the California National Primate Research Center (Davis, CA) were used for these experiments. All experimental procedures followed a protocol approved by the UCSF Institutional Animal Care and Use Committee and were conducted in accordance with the ARVO Statement on the Use of Animals in Ophthalmic and Vision Research.

Monkey 1, age 1 year, was used for an unrelated project. A week before his scheduled euthanasia, an injection of 2 mCi of [<sup>3</sup>H]proline (PerkinElmer) was made into the left eye. The animal was anesthetized with ketamine HCl (15 mg/kg intramuscularly) and the pupil was dilated with 1% cyclopentolate HCl and 2.5% phenylephrine HCl. After 10 minutes of ocular massage to soften the globe, topical anesthesia was applied with 1% proparacaine HCl. The tracer, dissolved in 50 µL of sterile saline, was injected into the midvitreal. Inspection afterward with an indirect ophthalmoscope showed no injury to the eye. The goal of this experiment was to reconstruct the complete pattern of input from one eye to the superior colliculus using the classic approach of tritium autoradiography.

Monkey 2, age 4 years, received an injection of cholera toxin subunit B into each eye, following the same procedures used in monkey 1. Cholera toxin subunit B Alexa Fluor 488 was injected into the right eye and cholera toxin subunit B Alexa Fluor 594 was injected into the left eye (ThermoFisher Scientific, Waltham, MA). Each injection consisted of 500 µg of tracer dissolved in 50 µL of sterile saline containing 5% dimethyl sulfoxide.<sup>6</sup>

After a survival time of 1 week for tracer transport, the animals were euthanized with pentobarbital (150 mg/kg). A liter of normal saline was perfused via the left ventricle followed by a liter of 4% paraformaldehyde in 0.1 M phosphate buffer solution.

### Histological Processing

The brainstem from each animal was removed and placed into 4% paraformaldehyde in 0.1 M phosphate buffer solution with 30% sucrose for cryoprotection. In monkey 1, serial sections were cut perpendicular to the surface of the midbrain at 25 µm on a freezing microtome.

The sections were defatted for autoradiography, coated with NTB emulsion (Carestream Health, Rochester, NY), exposed in the dark for 2 weeks, processed with D-19 developer (Photographer's Formulary, Condon, MT), and cover-slipped with Permout. In monkey 2, serial sections for epifluorescence microscopy were cut at 40 µm and cover-slipped with a mounting media consisting of 80% glycerin/20% Tris buffer, 0.1 M, pH 8.5.

### Image Analysis

For monkey 1, autoradiographic sections were examined in lightfield and darkfield in an Olympus SZH10 stereomicroscope and photographed with a Spot Flex CCD camera (Spot Imaging, Sterling Heights, MI). The 160 colliculus sections were analyzed over a rostrocaudal distance of 4 mm.

For monkey 2, sections were examined in a Zeiss Axio-phot microscope (Carl Zeiss Meditec, Jena, Germany) with a 2.5× Plan-Neofluar objective. Alexa Fluor 488 was visu-

alized with the Chroma ET-EGFP(FITC/Cy2) filter set and Alexa Fluor 594 with the Chroma ET-CY3-TRITC filter set. Photographs were captured with a Spot Insight CMOS camera. Images taken with the two filter sets were imported into Photoshop (Adobe, San Jose, CA) and combined using the difference blending mode function. Trapped air bubbles were removed using the spot healing tool. The 84 serial sections, each 40-µm thick, were aligned by centering each on the aqueduct of Sylvius and the surface cleft between the colliculi. The image stack was imported into ImageJ (National Institutes of Health) and converted into a rotatable volume by using the three-dimensional viewer plug-in.

To determine the periodicity of the input to the superior colliculus, the column pattern in monkey 2 was analyzed using a power spectral density function in Igor Pro (WaveMetrics, Portland, OR) to generate a periodogram. A total of five representative regions each measuring 0.75 mm<sup>2</sup> were sampled.

## RESULTS

**Figure 1** shows the distribution of autoradiographic label in the superior colliculus of monkey 1 after [<sup>3</sup>H]proline injection into the left eye. Silver grains are densest in a thin band, generally less than 100 µm thick, close to the midbrain surface. A second, fainter tier is concentrated at a depth of 350 to 500 µm, in the stratum opticum. It contains linear streaks of label corresponding with the horizontal trajectory of axons, and punctate deposits representing terminals. In both colliculi, overall labeling intensity diminishes gradually with increasing distance from the midline.

As described originally by Hubel et al.,<sup>2</sup> input from the injected eye forms a mottled pattern, with bright clumps of label separated by darker zones. The grain-rich clumps are more distinct in the superior colliculus ipsilateral to the injected eye.<sup>2</sup> Throughout the entire stratum griseum superficiale and the stratum opticum, the density of silver grains far exceeds the background level present in the rest of the tissue section. It is clear from the use of only a single label, therefore, that input from the two eyes to the superior colliculus must overlap partially.

**Figure 2** shows a series of 16 sections spaced every 250 µm from the rostral to caudal pole of the superior colliculus. Viewing the ensemble, it is evident that the contralateral (right) side is labeled more strongly. To quantify this asymmetry, the density of the label in the portion of each section containing the superior colliculus was measured. Labeled regions outside the superior colliculus (e.g., the nucleus of the optic tract, pretectal olivary nucleus) were excluded. A histogram was compiled, composed of the gray-scale pixel values contained in all 16 images (Supplementary Fig. 1A). It had a bilobed distribution, with a sharp peak corresponding with white, unlabeled portions of the sections and a low, broad peak representing the darker autoradiographic signal. The histogram was thresholded at the trough between the peaks and the light pixels representing areas lacking signal (gray-scale values of >220) were ignored. The remaining histogram, weighed by gray-scale value, was compared between the contralateral and ipsilateral sides (Supplementary Fig. 1B). The ratio of contralateral/ipsilateral autoradiographic signal pixel strength was 1.47:1. This ratio corresponds with a weighting of 60%/40%, similar to the predominance of the contralateral eye in the primary visual cortex beyond an eccentricity of 8°. <sup>8</sup> One cannot, however,

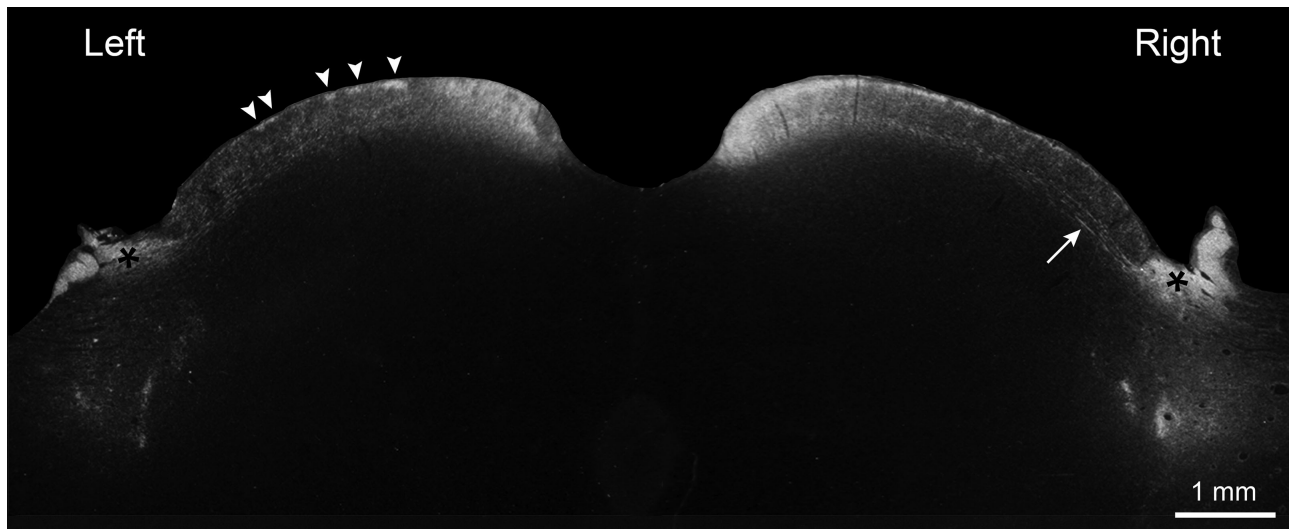


**FIGURE 1.** Autoradiograph from monkey 1 viewed in darkfield showing [ $^3\text{H}$ ]proline from the left eye aggregated into irregular columns (*arrowheads*), especially at the surface of the superior colliculus. The label is most dense medially. Horizontally oriented axons are visible in the stratum opticum (*arrow*). The nucleus of the optic tract (\*) is visible bilaterally.

extrapolate directly from image pixel density to the number of synapses made by retinal ganglion cell terminals.

The sections exhibit a medial to lateral decrement in the strength of the autoradiographic signal beginning about 60 sections, or 1.5 mm, from the caudal pole of the tectum. In [Figure 2](#), this effect becomes apparent starting with the sixth section from the caudal end. A comparison of the coronal autoradiographs with the colliculus retinotopic map reveals that the loss of signal strength is correlated with eccentricity ([Fig. 3](#)). Owing to a tilting of the visual field map with respect to the midbrain's sagittal plane, the lateral portion of each section is located much closer to the representation of the fovea. The gradual decrease in the density of silver grains toward the lateral edges of the more anterior sections reflects a weakening of retinal input to the more central portion of the visual field representation.

In the primary visual cortex, previous studies have shown a sharply defined gap in autoradiographic label contralateral to the [ $^3\text{H}$ ]proline-injected eye that corresponds with a hole left by the optic disc.<sup>9,10</sup> In the superior colliculus, we observed hints of a label sparse zone around section 70 of 160 from the caudal end ([Fig. 2](#), region marked by "?"), but could not identify an optic disc representation with any confidence. The same was true on the ipsilateral side; there was a solid zone of label that might correspond to the optic disc representation, but it was the same size as other scattered clumps of silver grains. Given that receptive fields at  $15^\circ$  eccentricity have a diameter of  $5^\circ$ , one would expect receptive field scatter to blur the boundaries of any region corresponding to the blind spot.<sup>11</sup>

[Figure 4A](#) shows a coronal section through the superior colliculus of monkey 2 labeled by cholera toxin subunit B injection into each eye. There is a uniform field of intense label in the medial portion of each superior colliculus, corresponding with the monocular crescent representation of the contralateral eye, because this is a relatively caudal section. Moving laterally, the label from the other eye becomes visible, and predominates at a different depth from the surface, giving a tiered appearance to the ocular inputs. Wherever the two labels are concentrated in the same portion of the

superior colliculus, they avoid each other. Gaps in one label are filled by clumps of the other label ([Figs. 4B–D](#)). There is some overlap, signified by a few scattered yellow pixels, but the prevailing tendency is for inputs from the two eyes to interdigitate.

[Figure 5A](#) shows a complete stack of serial cross-sections through the superior colliculus, viewed from above and behind, at approximately the same perspective as [Figure 3B](#). The reconstruction captures the label present on the dorsal surface of the midbrain. The posteromedial aspect of each colliculus is labeled robustly by the contralateral eye. Moving anteriorly and laterally towards more central visual field, the opposite eye becomes more strongly represented at the surface ([Fig. 5](#)). Where both labels are present, lacunae in one eye's label are filled by input from the other eye. Moving still further along the horizontal meridian, toward the foveal representation, the strength of label from both eyes diminishes sharply. This trend is consistent with the data from autoradiography, which also show relative weakening of signal in more central portions of the visual field map ([Fig. 2](#)). The decrease is even more striking in the fluorescent label, compared with the [ $^3\text{H}$ ]proline label, for unknown reasons. A failure of uptake from the macula was not responsible, because an examination of the lateral geniculate nuclei showed no difference in signal strength in sections representing the peripheral versus central visual field.

A Fourier analysis of the periodicity of the column pattern, tested where ocular inputs interdigitate extensively ([Fig. 5A](#)) in the midperiphery of the visual field representation, yielded a mean value of  $4.22 \pm 1.1$  cycles/mm ( $n = 5$  zones sampled). This corresponds with a mean width for a single eye's columns of  $118 \mu\text{m}$ .

The columnar organization of ocular input is readily apparent, whether the superior colliculus is labeled by [ $^3\text{H}$ ]proline or cholera toxin subunit B. In contrast, the laminar segregation of ocular inputs is difficult to appreciate in autoradiographs, because only one eye is labeled ([Figs. 1](#) and [2](#)). However, once each eye's input is labeled with an independent tracer, it emerges as a striking feature ([Fig. 5B](#)).



**FIGURE 2.** Every 10th autoradiograph from monkey 1 viewed in brightfield showing clumps of label from the rostral to caudal pole (the top two sections contain stratum opticum but not stratum griseum superficiale). The seventh section from the top (\*) is shown in [Figure 1](#). The asterisk is placed at 20° eccentricity. The asterisk in the fifth section from the bottom is also placed at 20° eccentricity; therefore, the intensity of silver grains at both sites is similar. At eccentricities below 10° the autoradiographic label weakens, accounting for the fall off in grain density in the lateral portion of more anterior sections. ? = possible location of the left eye's optic disc representation.

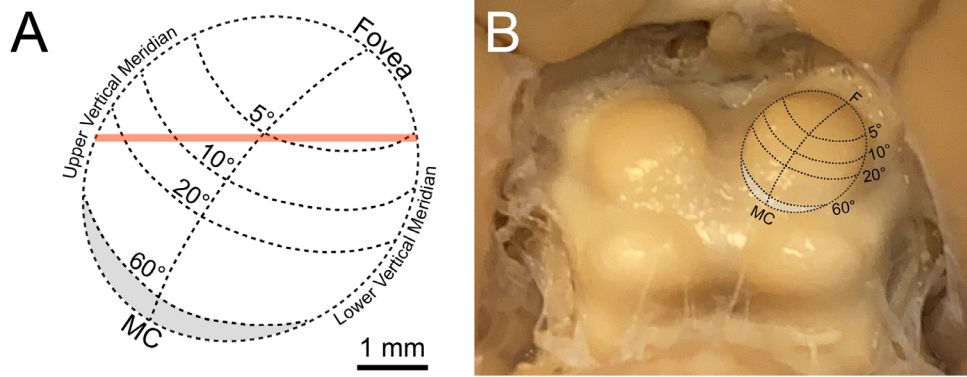


**FIGURE 3.** Retinotopic map of the right superior colliculus. (A) The dashed line between the fovea and monocular crescent (MC) represents the horizontal meridian. The central 10° occupies nearly half the structure. Pink line corresponds to the section shown in Figure 1. (B) Map superimposed on the superior colliculus of a fixed specimen. Oblique orientation of the horizontal meridian means that the lateral portion of any coronal section represents more central visual field.

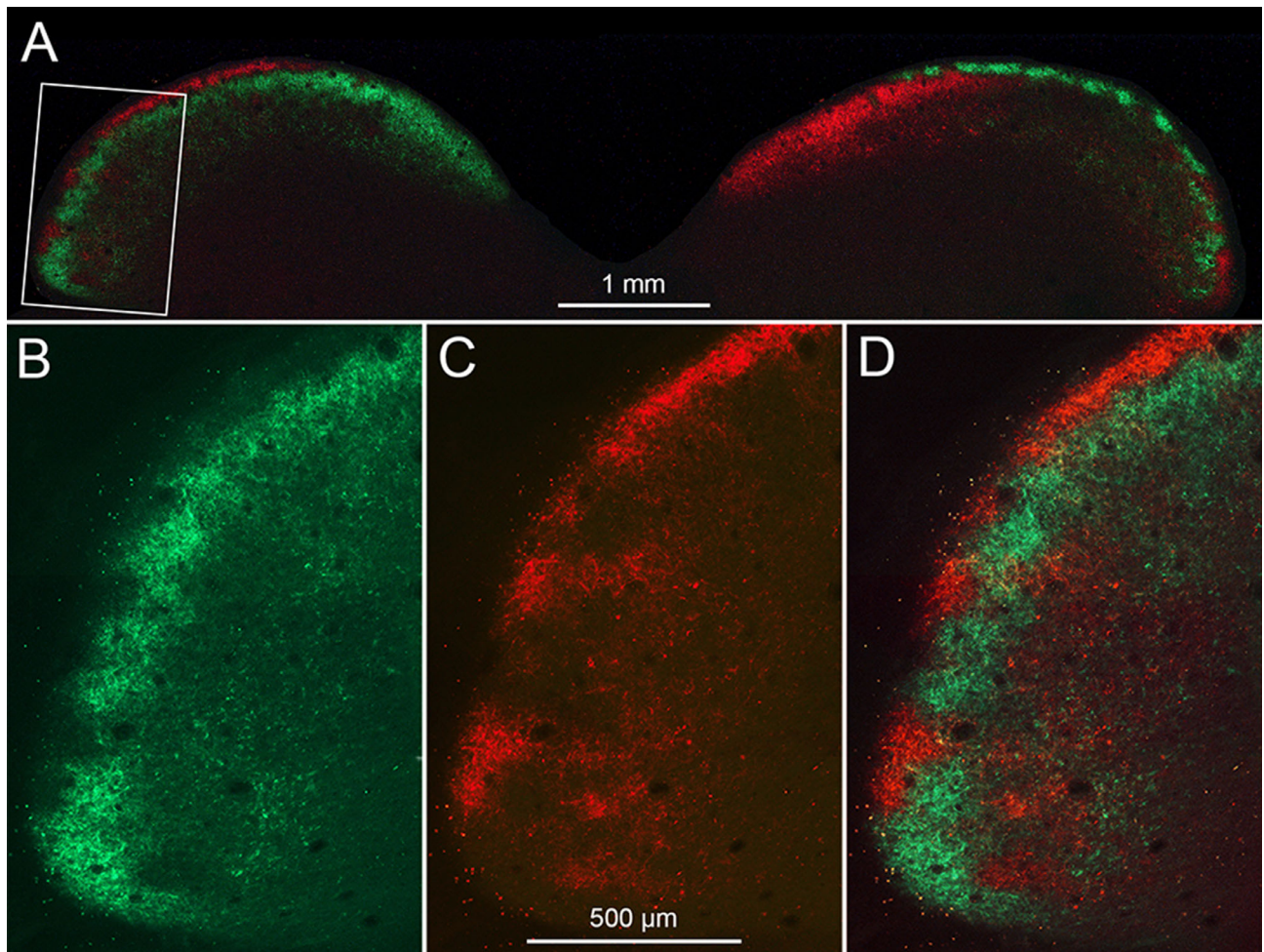


**FIGURE 4.** Cholera toxin subunit B labeling in monkey 2. (A) Coronal section near the caudal end of the superior colliculus showing input from the right eye (green, Alexa Fluor 488) and the left eye (red, Alexa Fluor 594). The solid medial label corresponds with the monocular crescent of each eye. (B) Boxed region in (A), showing Alexa Fluor 488. (C) Same region, showing Alexa Fluor 594. (D) Labels combined with the Photoshop difference blending mode function, showing that ocular inputs from the eyes are mainly interdigitated into separate columns and sublayers.

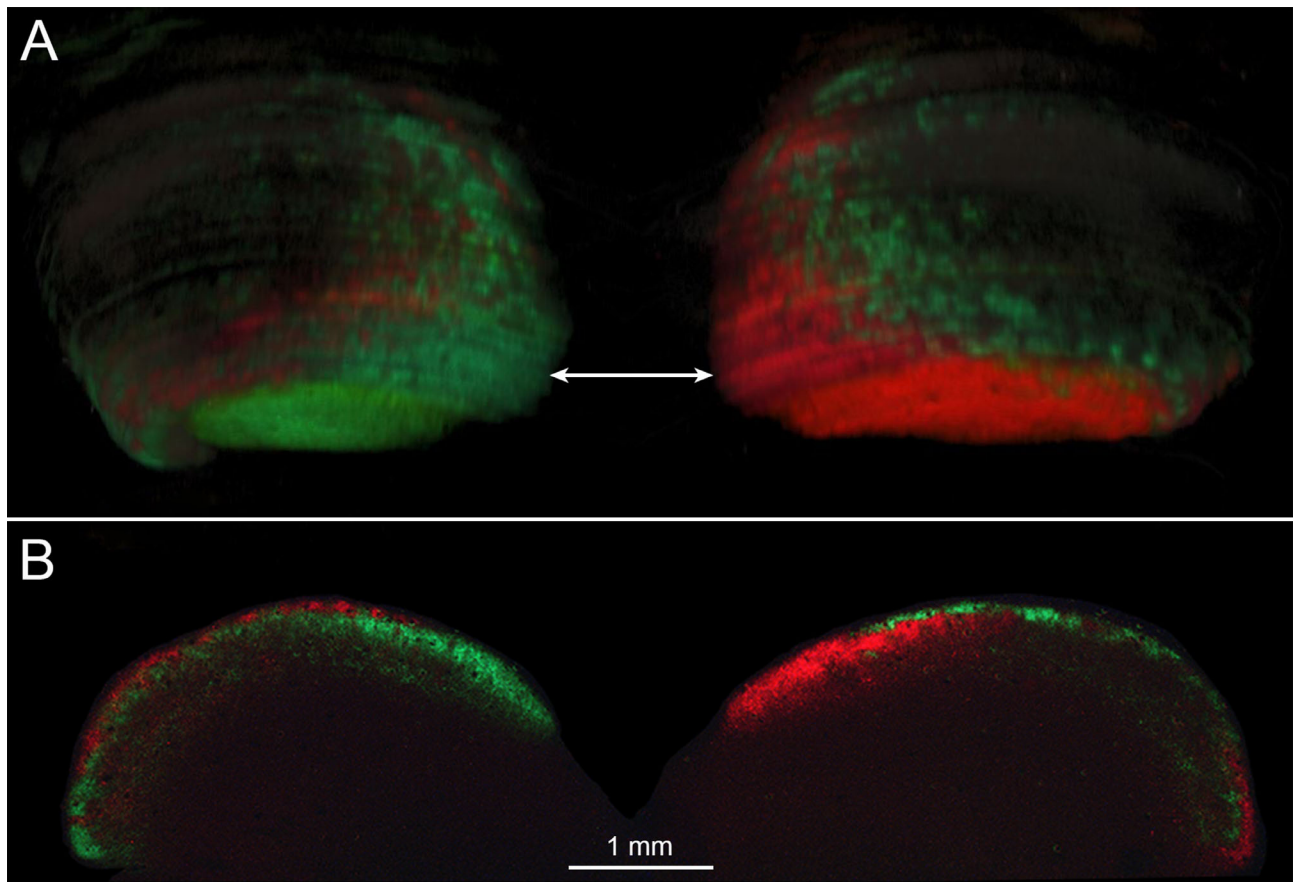


**FIGURE 5.** A three-dimensional reconstruction of 84 serial sections in monkey 2. **(A)** Superior colliculus viewed posteriorly from the same vantage point as in [Figure 3](#). Label at the surface of the tectum (*green* = right eye, *red* = left eye) is visible. The contralateral eye is dominant posteromedially, but progressing along the horizontal meridian the ipsilateral eye begins to appear at the surface. Where both labels are present superficially, they form interdigitated columns. Note the weaker label in the central 10° (*dark regions*). The *double-headed arrow* denotes the single section below. **(B)** Single coronal section from the reconstruction above, showing laminar and columnar interdigitation of signal from each eye.

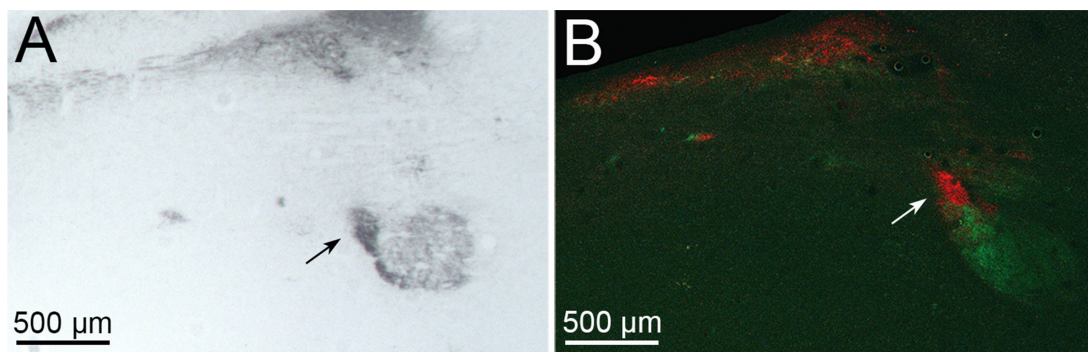


**FIGURE 6.** Pretectal olivary nucleus. **(A)** Right olivary nucleus from monkey 1, at the anterior end of the superior colliculus, just below the nucleus of the optic tract. Note the greater density of the label at the superomedial apex (*arrow*) after [<sup>3</sup>H]proline injection into the left eye. **(B)** The same region in monkey 2, showing cholera toxin subunit B Alexa Fluor 594 from the left eye concentrated at the superomedial apex (*arrow*). It reveals that the more intense region of label in **(A)** is due to partial segregation of ocular input to the olivary nucleus.

Curiously, ocular inputs to the nucleus of the optic tract and the olivary nucleus were also segregated partially. [Figure 6A](#) shows the right olivary nucleus of monkey 1 labeled by [<sup>3</sup>H]proline injection into the left eye. The entire nucleus is

filled, but the density of silver grains is greater at the superomedial apex. [Figure 6B](#) shows the right olivary nucleus of monkey 2. The strongest input from the left eye is also present at the superomedial apex of the nucleus.

## DISCUSSION

The principal finding in this study is that—just as surmised by Hubel et al.<sup>2</sup>—the input from each eye to the superior colliculus terminates in segregated, alternating clumps, mainly within the stratum griseum superficiale. The alternative possibility, that input from the eyes overlaps within clumps separated by unlabeled regions, is rejected by the dual fluorophore cholera toxin subunit B tracer experiment in monkey 2. The interdigitation of the eyes in the superior colliculus is reminiscent of the ocular dominance columns in the primary visual cortex. However, the columns in the primary visual cortex are far wider, more regular, and much better segregated. Consequently, most cells in the cortex are dominated by one eye, whereas in the superior colliculus virtually all cells are activated equally by both eyes, even when cortical input is silenced.<sup>12–14</sup> Neurons in the superficial layers of the superior colliculus have dendritic fields that are large relative to clumps of retinal input.<sup>15</sup> Their dendrites are able to receive signals from both eyes by passing through clusters of retinal axon terminals from the right eye and from the left eye.

In addition to columnar segregation, retinal afferents showed pronounced laminar segregation within the superior colliculus. This property was mentioned by Hubel et al.,<sup>2</sup> who observed the contralateral eye input to be more continuous superficially, with the ipsilateral input in clumps displaced to a deeper level. This arrangement was observed in portions of the superior colliculus of monkey 2, especially in the far periphery near the temporal crescent representation (Fig. 4A). In the midperiphery, the eyes flipped relative depth, with the ipsilateral retinal input usually rising closer to the surface (Fig. 5B), as shown previously by Pollack and Hickey.<sup>5</sup> The combination of both laminar and columnar interdigitation meant that the clumps of input serving each eye sometimes formed a scattered, irregular check-board pattern in cross-sections (Fig. 4D).

A conspicuous, unexplained feature of the retinocollicular projection is that it is weighted strongly to the peripheral visual field representation. This bias is present whether ocular input is labeled with [<sup>3</sup>H]proline or cholera toxin subunit B (Fig. 2, Fig. 5). Perhaps it is an artifact, owing to the fact that the ganglion cells in the macula are stacked densely, giving them more limited access to a tracer injected into the vitreous. Such an impediment would result in an apparently weaker input from the central retina to the superior colliculus. Evidence counter to this explanation is provided by studies showing that retinal lesions produce far fewer degenerating terminals at the rostral pole of the superior colliculus.<sup>16,17</sup> This experimental approach is not subject to the potential pitfall of eccentricity-dependent tracer uptake. Near the fovea only 6% of ganglion cells are labeled by retrograde tracer injection into the superior colliculus, compared with an overall mean of 10%, confirming the relative weakness of the central retinal projection.<sup>1</sup>

One cannot be sure how sharply direct retinal input decreases as a function of decreasing distance from the center of gaze, because the magnification of the macula in the superior colliculus is still uncertain. Measurements of the Cynader and Berman map show that they allocated 54% of the superior colliculus to the central 10°, whereas Robinson assigned only 36%.<sup>12,18</sup> We apportioned 47% to the central 10° (Fig. 3), based on chamber grid coordinates from a recent series of recordings, which showed that strabismus does not alter map topography in the superior colliculus.<sup>19</sup> The rela-

tive magnification of the macula in the superior colliculus and the primary visual cortex may be essentially equal.<sup>20</sup> If so, a decrease in retinal input to the superior colliculus occurs within a zone that corresponds to the macular representation. Parasol cells and smooth cells project to both the superior colliculus and the lateral geniculate nucleus, via branching axons.<sup>21,22</sup> Accordingly, one would predict that in the macula, fewer such retinal cells sport a branch to the superior colliculus.

Two major questions remain unanswered, namely, what is the function of the direct retinal input to the superior colliculus and why is it segregated by eye? The superior colliculus integrates sensory information to orient motor action toward salient stimuli.<sup>23–28</sup> The generation of saccades to visual targets is among its most prominent motor outputs. If direct retinal input is involved in this function, then the fact that the peripheral projection is more extensive implies that it plays a more important role in the execution of large saccades compared with small saccades. This premise could be tested by selectively ablating the direct retinal input to the superior colliculus.

With regard to segregation of the ocular inputs in the superior colliculus, we have asserted previously that columnar organization is of no functional importance in the nervous system.<sup>29</sup> This view is supported by the observation in the olivary nucleus of partial segregation of ocular inputs (Fig. 6).<sup>6</sup> One can argue plausibly that columns serve a vital role in the superior colliculus or primary visual cortex (although this role remains to be elucidated). The olivary nucleus, in contrast, is a simple pupil driver. The pupils always fluctuate identically in diameter, so no functional advantage can derive from segregating ocular input to the olivary nucleus. It seems that axon terminals from the two eyes are mutually repellant within a variety of structures that receive direct input, perhaps for reasons unrelated to any purpose that such segregation serves in the mature nervous system.

## Acknowledgments

Supported by grants EY029703 (J.C.H.) and EY02162 (Vision Core Grant) from the National Eye Institute and by an unrestricted grant from Research to Prevent Blindness. The California National Primate Research Center is supported by a Base Grant from the NIH Office of the Director, OD011107.

Disclosure: **M.D. Dilbeck**, None; **Z.R. Spahr**, None; **R. Nanjappa**, None; **J.R. Economides**, None; **J.C. Horton**, None

## References

1. Perry VH, Cowey A. Retinal ganglion cells that project to the superior colliculus and pretectum in the macaque monkey. *Neuroscience*. 1984;12:1125–1137.
2. Hubel DH, LeVay S, Wiesel TN. Mode of termination of retinotectal fibers in macaque monkey: an autoradiographic study. *Brain Res*. 1975;96:25–40.
3. Wassle H, Illing RB. The retinal projection to the superior colliculus in the cat: a quantitative study with HRP. *J Comp Neurol*. 1980;190:333–356.
4. Hofbauer A, Dräger UC. Depth segregation of retinal ganglion cells projecting to mouse superior colliculus. *J Comp Neurol*. 1985;234:465–474.
5. Pollack JG, Hickey TL. The distribution of retino-collicular axon terminals in rhesus monkey. *J Comp Neurol*. 1979;185:587–602.

6. Muscat L, Huberman AD, Jordan CL, Morin LP. Crossed and uncrossed retinal projections to the hamster circadian system. *J Comp Neurol*. 2003;466:513–524.
7. Vigouroux RJ, Duroure K, Vougnny J, et al. Bilateral visual projections exist in non-teleost bony fish and predate the emergence of tetrapods. *Science*. 2021;372:150–156.
8. Horton JC, Hocking DR. Intrinsic variability of ocular dominance column periodicity in normal macaque monkeys. *J Neurosci*. 1996;16:7228–7239.
9. LeVay S, Wiesel TN, Hubel DH. The development of ocular dominance columns in normal and visually deprived monkeys. *J Comp Neurol*. 1980;191:1–51.
10. Horton JC, Hocking DR. An adult-like pattern of ocular dominance columns in striate cortex of newborn monkeys prior to visual experience. *J Neurosci*. 1996;16:1791–1807.
11. Schiller PH, Stryker M. Single-unit recording and stimulation in superior colliculus of the alert rhesus monkey. *J Neurophysiol*. 1972;35:915–924.
12. Cynader M, Berman N. Receptive field organization of monkey superior colliculus. *J Neurophysiol*. 1972;35:187–201.
13. Goldberg ME, Wurtz RH. Activity of superior colliculus in behaving monkey. I. Visual receptive fields of single neurons. *J Neurophysiol*. 1972;35:542–559.
14. Schiller PH, Stryker M, Cynader M, Berman N. Response characteristics of single cells in the monkey superior colliculus following ablation or cooling of visual cortex. *J Neurophysiol*. 1974;37:181–194.
15. May PJ. The mammalian superior colliculus: laminar structure and connections. *Prog Brain Res*. 2006;151:321–378.
16. Lund RD. Synaptic patterns in the superficial layers of the superior colliculus of the monkey, *Macaca mulatta*. *Exp Brain Res*. 1972;15:194–211.
17. Wilson ME, Toyne MJ. Retino-tectal and cortico-tectal projections in *Macaca mulatta*. *Brain Res*. 1970;24:395–406.
18. Robinson DA. Eye movements evoked by collicular stimulation in the alert monkey. *Vision Res*. 1972;12:1795–1808.
19. Economides JR, Rapone BC, Adams DL, Horton JC. Normal Topography and Binocularity of the Superior Colliculus in Strabismus. *J Neurosci*. 2018;38:173–182.
20. Chen CY, Hoffmann KP, Distler C, Hafed ZM. The foveal visual representation of the primate superior colliculus. *Curr Biol*. 2019;29:2109–2119 e2107.
21. Crook JD, Peterson BB, Packer OS, et al. The smooth monostratified ganglion cell: evidence for spatial diversity in the Y-cell pathway to the lateral geniculate nucleus and superior colliculus in the macaque monkey. *J Neurosci*. 2008;28:12654–12671.
22. Crook JD, Peterson BB, Packer OS, Robinson FR, Troy JB, Dacey DM. Y-cell receptive field and collicular projection of parasol ganglion cells in macaque monkey retina. *J Neurosci*. 2008;28:11277–11291.
23. Wurtz RH, Albano JE. Visual-motor function of the primate superior colliculus. *Annu Rev Neurosci*. 1980;3:189–226.
24. Horwitz GD, Newsome WT. Separate signals for target selection and movement specification in the superior colliculus. *Science*. 1999;284:1158–1161.
25. Schiller PH. The superior colliculus and visual function., *The Handbook of Physiology, Volume III*. New York: Wiley; 1984:457–505.
26. Gandhi NJ, Katnani HA. Motor functions of the superior colliculus. *Annu Rev Neurosci*. 2011;34:205–231.
27. Song JH, McPeck RM. Neural correlates of target selection for reaching movements in superior colliculus. *J Neurophysiol*. 2015;113:1414–1422.
28. Basso MA, May PJ. Circuits for action and cognition: a view from the superior colliculus. *Annu Rev Vis Sci*. 2017;3:197–226.
29. Horton JC, Adams DL. The cortical column: a structure without a function. *Philos Trans R Soc Lond B Biol Sci*. 2005;360:837–862.